Desalination and Water Treatment
www.deswater.com

doi: 10.5004/dwt.2021.26917

217 (2021) 431–441
March

Adsorption of Crystal violet dye with cellulose derived from bitter gourd waste

Linda B.L. Lim[a,*], Namal Priyantha[b], Iqbal Fitri Kamaludin[a], Nur Afiqah H. Mohamad Zaidi[a], A.P.G.M.V. Samaraweera[b]

[a]*Chemical Sciences, Faculty of Science, Universiti Brunei Darussalam, Jalan Tungku Link, Gadong, Negara Brunei Darussalam, Tel. 00-673-8748010; emails: linda.lim@ubd.edu.bn (L.B.L. Lim), iqbalphk@gmail.com (I.F. Kamaludin), afhazirah@gmail.com (N.A.H. Mohamad Zaidi)*
[b]*Department of Chemistry, University of Peradeniya, Peradeniya, Sri Lanka, emails: namal.priyantha@yahoo.com (N. Priyantha), madushanka10@gmail.com (A.P.G.M.V. Samaraweera)*

Received 15 May 2020; Accepted 11 December 2020

ABSTRACT

Momordica charantia, or more commonly known as bitter gourd, has shown numerous health benefits, mainly decreasing the risk of diabetes. Nevertheless, the use of its inedible parts as an adsorbent toward different pollutive dyes has not been greatly explored through optimization, kinetics, and adsorption equilibrium studies. In this study, the cellulose derived from bitter gourd waste of pith and seeds (CBGW) was extracted and its adsorption characteristics were investigated with Crystal violet (CV) dye. It was found that the adsorption of CV by CBGW favors the pseudo-second-order kinetics. Changing the medium pH has little or no effect toward CV removal, indicating that the CBGW is resilient under various pH conditions. The presence of salts also generally did not very much affect the removal of CV. When compared to many reported adsorbents, CBGW exhibited superior adsorption capacity for CV dye, as seen by its high maximum adsorption capacity of 1,565 mg g^{-1} (Langmuir) and 2,407 mg g^{-1} (Sips). Spent CBGW was able to be regenerated and reused, further adding to its value as a possible candidate in wastewater application.

Keywords: Momordica charantia; Adsorption; Kinetics; Equilibrium; Salts

1. Introduction

As the world advances in terms of health and technology, so does the increasing rate of the growing population leading to the accumulation of waste, which is being deposited in many countries at alarming rates. For example, Brazil (Rio de Janeiro) deposits more than 10,000 tons of waste each day [1]. In Brunei Darussalam, the generation of waste is one of the highest per capita in the region. In 2014, an average Bruneian generates about 1.4 kg of wastes per day [2]. Seen as a huge problem that needs to be solved quickly, there are certain measurements that can be made to help deal with this issue. Public awareness regarding the importance of keeping a healthy environment can be done; however, the result to the action can be miniscule. Due to this fact, other measurements have to be made to reduce such problems.

Dyes have become an integral part in human life. They are very widely used in the contemporary world to add different shades of colors to materials ranging from fabrics to food, so that the materials can look more appealing from the consumer's perspective. Most of the natural dyes are safe to use and do not bring harm to the environment. However, in the process of making these dyes, other ingredients such as hematein and hematoxylin present in

* Corresponding author.

some sources such as logwood are toxic [3]. Metals, such as copper and iron, are also introduced in the production of some natural dyes, so that it could attach itself better to some materials such as fabrics for long lasting effect. Nowadays, synthetic dyes are preferred over natural dyes to be used in industries, mainly due to faster production in large quantities in a wide range of colors as compared with natural dyes. However, the downside of synthetic dyes is that transition metals are used in manufacturing them to produce different spectrum of colors, making them harmful to the environment.

It is stated that as much as 200,000 tons of dyes are annually lost as liquid waste [4]. Textiles industries usually used many different types of dyes, and leachates formed from such industries, if disposed of without proper treatment, could pose detrimental effects on the environment. The presence of dyes in water could cause decrease in light penetration to aquatic systems, resulting in lack of photosynthesis in aquatic biological plants which in turn results in less oxygen to be distributed to other aquatic life, causing disturbance to the ecosystem [5,6]. Another issue to be considered is that the quality of textiles dyes depends on how strongly they are adsorbed on fabrics and on non-biodegradability, and hence, they are not easily removable. This should thus be considered in designing treatment plants for dyes as well as in regeneration efforts.

There are multiple methods to remove environmental pollutants in water, specifically dyes. Some common methods include reverse osmosis, coagulation, and chemical precipitation and adsorption [7,8]. Among them, adsorption by natural adsorbents has become attractive owing to its unique advantages, such as relatively low-cost, simplicity, and environmentally friendliness [9]. The performance of natural adsorbents can be improved in many directions. The selectivity of an adsorbent can be controlled by proper selection of experimental and process variables [10]. The surface of adsorbents can be modified by suitable chemical reagents to introduce more effective characteristics [11]. Efficiency of adsorbents can thereby be enhanced. Although there is an enormous amount of literature available on attempts made to make use of natural adsorbents [12], the above developments have not been much attended to.

Momordica charantia (bitter gourd) is a member of the Cucurbitaceae family. Besides its use as a culinary ingredient, the plant also has medicinal properties, for example, the treatment of Type 2 diabetes mellitus [13]. Though they are quite useful in treating health problems, very few studies were conducted using the fruit for adsorbing environmental pollutants. One study on using its waste to adsorb Crystal violet (CV) dye reported an adsorption capacity of 261.8 mg g^{-1} [14]. Other reports indicate that the peroxidase of bitter gourd has good adsorption ability [15]. Pith and seeds of *M. charantia* are not eaten when cooking the bitter gourd and are thrown as waste. The adsorbate selected in this investigation is an industrial dye.

CV dye has a myriad number of uses in everyday life; in fingerprinting of electrophoresis in forensic studies, as a dying agent in paper industry and in the textiles industry. It is also known to have antibacterial properties [16]. Despite its many uses, there are many undesirable effects. For instance, chemical cystitis was observed when CV dye was used as a disinfectant and further, the dye could be toxic to mucosal membranes [17].

Cellulose is a hydrocarbon that consists of polysaccharides with β-1,4 glycosidic bonds, and it is the primary component in giving the plants its rigidity and structure due to it being the compound that creates the cell wall [18]. Numerous studies have shown cellulose to be a good adsorbent. In one study, dialdehyde micro-fibrillated cellulose/chitosan composite film was used to adsorb Congo red dye with a high percentage removal of 99.95% within 10 min [19]. Another example is the adsorption of malachite green on cellulose nanofibril aerogels with adsorption capacity of 212.7 mg g^{-1} [20]. Oxidized cellulose obtained using cellulose chromatography paper has shown a much higher adsorption capacity of 1,117.8 mg g^{-1} [21].

To date, the use of cellulose derived from *M. charantia* (bitter gourd) waste of pith and seeds (CBGW) as an adsorbent has not been previously reported. Hence, the aim of this investigation was to perform detailed investigation on adsorption characteristics of CBGW through optimization, adsorption equilibrium, and kinetic experiments. Adsorption characteristics of CBGW toward CV dye were compared with those of bitter gourd waste (BGW) and other reported adsorbents to demonstrate the superior ability of CBGW. The ability to produce a low cost and yet highly effective adsorbent could thus be one potential solution for the treatment of industrial effluents containing CV dye.

2. Methodology

2.1. Preparation of cellulose derived BGW

The BGW that was used in this investigation consisted of pith and seeds. Samples of bitter gourd were randomly purchased from local markets in the Brunei-Muara District of Brunei Darussalam. Each bitter gourd was split open, and the inedible parts of pith and seeds were scraped off the meat of bitter gourd and collected as the adsorbent material. The fresh adsorbent was allowed to dry for a period of one week in an oven at 55°C, monitoring the mass of the sample to ensure that no water remained in the dried sample. After collecting the dried BGW, it was then milled to a finer form and sieved using a laboratory metal sieve to 380 μm to obtain fine powder form.

The dried BGW powder was processed further adapting the method used for extracting cellulose as outlined elsewhere [22]. Briefly, BGW (20.0 g) was placed in a 1.0 L round bottom flask, and to this were added 10 mL of 69% nitric acid and 100 mL of concentrated acetic acid. The mixture was refluxed for 4.0 h at 120°C, after which the contents were allowed to cool to room temperature and then gravity filtered. Thereafter, the residue was collected and allowed to dry in an oven to a constant weight. The dried samples were milled to fine powder and sieved again with a 380 μm laboratory sieve. The dried cellulose derived from bitter gourd waste (CBGW) powder was kept in an air tight plastic bag to prevent exposure to the surrounding until ready to be used.

2.2. Investigation of contact time

An aliquot of 10 mL of 500 mg L^{-1} of CV dye was separately added into conical flasks each containing 20 mg

of CBGW. Each sample was shaken at 250 rpm at ambient temperature using a shaker for a total period of 240 min. After every 30 min, one flask was removed from the shaker and the mixture was filtered using a metal sieve. The filtrate was then analyzed for its absorbance using the Thermo Scientific Genesys 20 (USA) UV-vis spectrophotometer set at wavelength 590 nm. When the concentration of the dye was beyond the linear dynamic range of detection, filtrates were diluted accordingly.

The percentage removal of dye was calculated by Eq. (1) below:

$$\%\ \text{Removal} = \frac{\text{Final concentration of CV}}{\text{Initial concentration of CV}} \times 100\% \quad (1)$$

Calibration curves were freshly constructed with standard solutions of the dye in the concentration range of up to 10 mg L^{-1} to obtain the concentration of the dye in each solution.

2.3. Effect of pH on adsorption of CV dye

Adsorption of CV dye by CBGW was investigated in solutions of different pH ranging from 2.0 to 10.0 as well as at untreated (ambient) pH of 5.55, in order to determine the optimum pH for adsorption studies. For this purpose, solutions of different pH were prepared using 1.0 M of HCl and/or NaOH. Thereafter, aliquots of 10.0 mL of 100 mg L^{-1} CV dye solution were separately prepared in solutions of each pre-determined pH and 20 mg of CBGW was added to each solution. The mixture was shaken for 210 min at the 250 rpm at ambient temperature. Each mixture was immediately filtered and the filtrate was diluted as necessary and analyzed for CV concentration.

2.4. Investigation of adsorption isotherms

For the investigation of adsorption isotherms, solutions of CV of the initial concentrations ranging from 10 to 3,000 mg L^{-1} were freshly prepared from stock solutions. All experiments were carried out in 1.0 g:500 mL adsorbent: adsorbate ratio, unless otherwise stated. The mixture was then shaken for 210 min at 250 rpm at ambient temperature. After shaking, the mixture was filtered, and the filtrate was analyzed for the concentration of CV based on a freshly constructed calibration curve.

The best fit adsorption model was also analyzed using five error functions, namely, average relative error (ARE), sum of the errors squared (ERRSQ), sum of the absolute errors (EABS), hybrid fractional error function (HYBRID), and chi square error (χ^2) which are shown in Table 1.

2.5. Investigation of adsorption kinetics

Adsorption kinetics was performed using freshly prepared solutions of CV of initial concentrations of 100 and 500 mg L^{-1} from stock solutions. For each measurement, 20 mg of CBGW was mixed with 10.0 mL of CV solution of the relevant concentration. Each mixture was shaken for a pre-determined time period, the suspension was immediately filtered and the filtrate was diluted as necessary and analyzed for CV concentration based on a freshly constructed calibration curve. Three min measurements were taken for the first 30 min period, then 10 min measurements were taken for the next 60 min period, and finally 30 min measurements were taken for the next 210 min period.

2.6. Effect of ionic strength on adsorption of CV dye

Stock solutions of 2.0 M solution of each of the salts, KNO_3, KCl, $NaNO_3$, and NaCl, and 1,000 mg L^{-1} of CV dye were prepared in distilled water. Solutions of CV at 100 mg L^{-1} in different salt concentrations using each of the four salt solutions were then prepared by mixing appropriate volumes of the above stock solutions and diluting with distilled water. Aliquots of 10.0 mL of each of the above solutions were separately mixed with 20 mg of CBGW, and shaken for 210 min at 250 rpm at ambient temperature. Each mixture was immediately filtered and the filtrate was diluted as necessary and analyzed for CV concentration.

2.7. Regeneration study of CBGW

The experiment was first started by shaking 1.0 g of adsorbent in 500 mL of 2,000 mg L^{-1} CV dye for 210 min at 250 rpm. The spent CBGW was then filtered and dried in an oven for a period of 24 h at 55°C while the absorbance of the filtrate was being measured. The ratio of dye added to the spent adsorbent was kept at 1 g:500 mL while for washing, the ratio was 1.0 g of spent adsorbent to 50 mL of washing reagents.

The dried dye loaded CBGW sample was weighed and split equally into five samples. Three samples were shaken with distilled water, one with 0.1 M HCl and one with 0.1 M

Table 1
Different error functions used in isotherm analysis

Type of errors	Equations
ARE	$\frac{100}{n}\sum_{i=1}^{n}\left\lvert\frac{q_{e,\text{meas}}-q_{e,\text{calc}}}{q_{e,\text{meas}}}\right\rvert_i$
ERRSQ	$\sum_{i=1}^{n}\left(q_{e,\text{meas}}-q_{e,\text{calc}}\right)_i^2$
HYBRID	$\frac{100}{n-p}\sum_{i=1}^{n}\left[\frac{\left(q_{e,\text{meas}}-q_{e,\text{calc}}\right)^2}{q_{e,\text{meas}}}\right]_i$
EABS	$\sum_{i=1}^{n}\left\lvert q_{e,\text{meas}}-q_{e,\text{calc}}\right\rvert$
χ^2	$\sum_{i=1}^{n}\frac{\left(q_{e,\text{meas}}-q_{e,\text{calc}}\right)^2}{q_{e,\text{meas}}}$

where $q_{e,\text{meas}}$, experimental value; $q_{e,\text{calc}}$, calculated value; n, number of data points in the experiment.

NaOH, for 120 min at 250 rpm. Thereafter, each suspension was filtered by gravity and washed thoroughly with distilled water until the filtrate became pale color. One part of the spent CBGW was quickly washed and rinsed with distilled water while another part was kept unwashed to be used as the control for comparison purposes. All the above residues were dried before carrying out the next cycle. The dried residue obtained from the above process was subjected to repetition of shaking and washing with the different solvents (distilled water acid and base) up to three cycles.

2.8. Determination of point of zero charge

To determine the point of zero charge of CBGW, 0.10 M KNO_3 solutions were prepared separately at different pH values and CBGW was added in 1 g:500 mL ratio. Each suspension was shaken for a period of 24 h at 250 rpm using a thermo shaker. Thereafter, samples were filtered using gravity filtration, and the pH of each filtrate was measured.

2.9. Characterization of CBGW

The surface morphology of the CBGW, before and after adsorption of CV dye, was obtained on model JSM-7610F field emission scanning electron microscopy (FESEM). Carbon coating was used to obtain the image of the surface. Agilent Cary 630 Fourier transform infrared (FTIR) spectrometer was used to study functional groups in the CBGW.

3. Results and discussion

3.1. Effect of contact time

The extent of removal of CV by CBCW, determined at different contact time periods, leads to the conclusion that the CBGW-CV system reaches equilibrium at 210 min, beyond which the extent of removal becomes constant. Rapid removal of ~66% CV dye was observed within the initial 30 min, as shown in Fig. 1. This could be due to the availability of active binding sites on the surface of CBCW thereby allowing the CV dye molecules to be quickly adsorbed onto CBCW. As time proceeds, with more dye molecules occupying and filling up these active sites, the rate of adsorption gradually decreases and eventually reaches equilibrium. This observation is similar to what was reported for unmodified BGW for the same adsorbate, CV [14].

3.2. Effect of pH on adsorption of CV dye

Effect of change in pH of the adsorbate medium containing 100 mg L^{-1} CV dye solution within the range from pH 2 to 12 on adsorption by CBGW is shown in Fig. 2. Attraction between the lone pairs on electronegative oxygen atoms of cellulose and positively charged N atom on CV dye is one possibility for removal of CV dye from solution by the solid adsorbent. Such attractions are much stronger in the cellulose extracted from BGW rather than untreated BGW. The difference between the extent of removal of 67% CV dye by CBGW and that of 30% by untreated BGW at ambient pH of 5.6 is thus explained [14]. The lower removal ability at acidic medium pH is probably due to competition between H_3O^+ and CV dye molecules. More importantly, as the extent of CV dye removal is not significantly changed beyond pH = 5.6, no adjustment of pH is necessary. The pH-independence of the CV dye removal is also a remarkable characteristic of CBGW as dye adsorption by many other reported adsorbents, such as *Artocarpus odoratissimus* skin [23], *M. charantia* [14], Sepia shells [24], and silver nanoparticles immobilized on activate carbon [25], are found to be pH-dependent. This property is an added advantage of potential use of CBWG as an adsorbent in wastewater treatment plants. Although the optimum pH in this study was found to be at pH 8 and 10 with 71% CV removal, nevertheless the performance of CBWG at pH 5.6 and 6 was compatible to that of the optimum, with 70% and 69% removal, respectively.

3.3. Adsorption isotherms

Isotherm models are curved models describing the retention of the dye towards an adsorbent. Therefore, the best isotherm model for a particular adsorbent–adsorbate system can be chosen based on three criteria, that is, the R^2 value closest to unity, lowest error values of isotherm

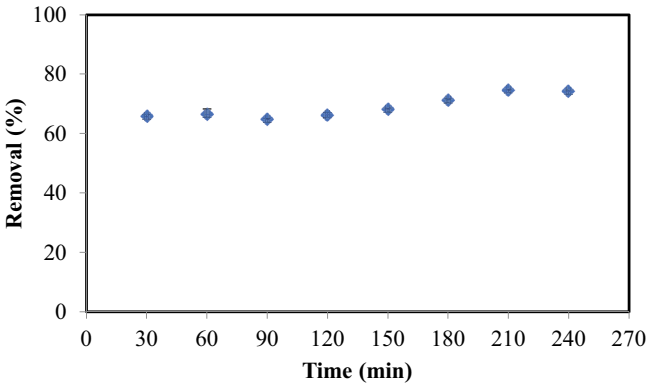

Fig. 1. Effect of contact time for the removal of CV dye.

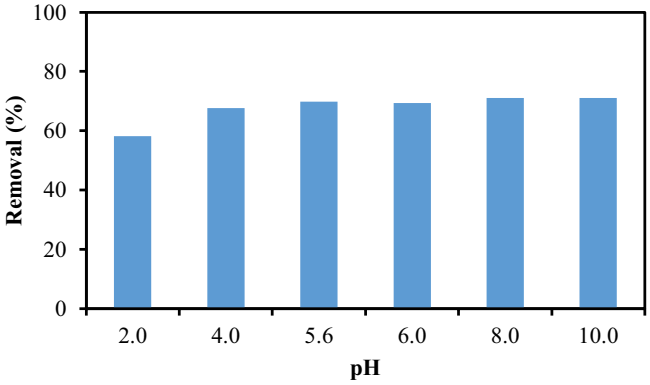

Fig. 2. Extent of removal of CV dye from 100 mg L^{-1} solutions by CBGW at different medium pH values (20.00 mL dye solution; 20 mg CBGW; 210 min shaking time; 250 rpm shaking speed).

model, and closest fit of model to experiment data. Six isotherm models used in this study to determine the most suitable adsorption characteristics of CV on CBGW are the Langmuir, Freundlich, Temkin, Dubinin–Radushkevich (D–R), Sips, and Redlich–Peterson (R–P) models, and their equations are as shown in Table 2.

The Langmuir model indicates uniform adsorption onto a homogenous solid surface and assumes that the adsorbent has a monolayer of adsorbate molecules on its surface [26]. The Freundlich adsorption isotherm is mostly used for heterogeneous systems where adsorption takes place in multi-layers on the sorbent's surface [27]. The Temkin model contains a factor for the adsorbent–adsorbate interactions. For this model, the values are not dependent toward the huge difference in the concentration values but rather the uniform distribution of binding energy [28]. The D–R model, often used for high solute activities within a range of concentrations. This model indicates the energy distribution toward a heterogeneous surface through the use of the Gaussian energy distribution [29]. The Sips isotherm is a combination of both the Langmuir and Freundlich models applied in heterogeneous systems. [30]. The R–P isotherm model is also a combination of both the Langmuir and Freundlich isotherms. This is a versatile model in adsorption science as it can be applied to either homogenous or heterogeneous systems [31].

The batch adsorption isotherm data obtained experimentally are presented in Fig. 3, together with the comparison with simulated data of the six isotherm models used. It is clear that, of the six models, large deviations from experiment data are observed for both the D–R and R–P models. This can be further confirmed by their R^2 values being the lowest and also by their high error values, especially for D–R isotherm (Table 3). Hence, these two models can be ruled out. Although the Freundlich model gives good R^2 value of 0.95, when compared to the experiment data, it overlaps with the R–P model showing huge deviation. Even though the Temkin model seemed to be closely fitted to the experiment data, its high ARE, HYBRID, and χ^2 error values indicate otherwise. Therefore,

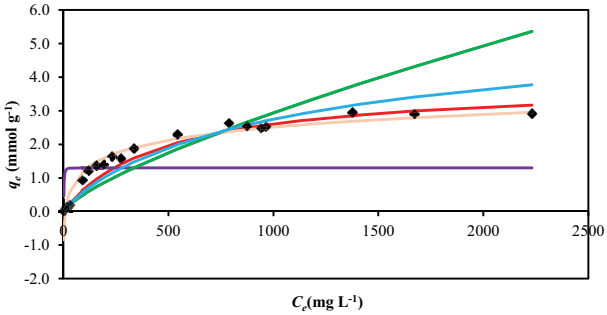

Fig. 3. Comparison of Langmuir (▬), Freundlich (▬), Temkin (▬), D–R (▬), R–P (▬), and Sips (▬) isotherm models for CBGW-CV system with experimental data (◆) (Freundlich and RP plot are identical).

Table 2
Six isotherm models used in this study

Isotherm model	Equation	Linearized equation
Langmuir	$Q_e = \frac{Q_m \cdot K_L C_e}{1 + K_L C_e}$	$\frac{C_e}{Q_e} = \frac{1}{K_L Q_m} + \frac{C_e}{Q_m}$
Freundlich	$Q_e = K_F C_e^{1/n}$	$\ln Q_e = \left(\frac{1}{n}\right)\ln C_e + \ln K_F$
Temkin	$Q_e = \frac{RT \cdot \ln\left(K_T C_e\right)}{b_T}$	$Q_e = \left(\frac{RT}{b_T}\right)\ln K_T + \left(\frac{RT}{b_T}\right)\ln C_e$
D–R	$Q_e = Q_m \cdot \exp\left(-B\left[RT\ln\left(1+\frac{1}{C_e}\right)\right]^2\right)$	$\ln Q_e = \ln Q_m - \left(-B\left[RT\ln\left(1+\frac{1}{C_e}\right)\right]^2\right)$
Sips	$Q_e = \frac{Q_m K_s C_e^{1/n}}{1 + K_s C_e^{1/n}}$	$\ln\left(\frac{Q_m}{Q_e} - 1\right) = -\ln K_s - \frac{1}{n}\ln C_e$
R–P	$Q_e = \frac{K_R C_e}{1 + a C_e^n}$	$\ln\left(\frac{K_R C_e}{Q_e} - 1\right) = \ln a + n\ln C_e$

where Q_e is the surface coverage at equilibrium at the adsorbate concentration of C_e; Q_m is the maximum adsorption capacity (monolayer coverage) of the sample and the K_L is the Langmuir constant; K_F and n are Freundlich constant and Freundlich intensity parameter (dimensionless); $b_T = RT\text{m}^{-1}$, and m is the gradient of the graph of q_e vs. lnC_e. The terms K_T is Temkin constant; R is universal gas constant and T is absolute temperature; B is D–R model constant; K_s is Sips model constant and $1/n$ is the Sips model exponent; K_R and a are (R–P) model constants and n (dimensionless) is an exponent whose value must lie between 0 and 1.

Table 3
Isotherm constants and error values for CBGW-CV system

Model	Values	ARE	ERRSQ	EABS	HYBRID	χ^2
Langmuir		12.25	0.94	3.14	2.87	3.61
q_{max} (mmol g^{-1})	3.84					
q_{max} (mg g^{-1})	1,565					
K_L (L $mmol^{-1}$)	0.00					
R^2	0.7244					
Freundlich		19.18	2.79	5.50	7.78	4.79
K ($mg^{(1-1/n)}$ $L^{1/n}$ g^{-1})	0.02					
n	1.33					
R^2	0.9461					
Temkin		275.16	1.77	4.60	200.24	48.09
K_T (L $mmol^{-1}$)	0.09					
b_T (J mol^{-1})	4,452.55					
R^2	0.8998					
D–R		473.52	18.77	18.03	481.74	118.33
q_{max} (mmol g^{-1})	1.30					
q_{max} (mg g^{-1})	529.96					
B (J mol^{-1})	1.40×10^{-06}					
E (kJ mol^{-1})	598.22					
R^2	0.6479					
Redlich–Peterson		18.88	2.74	5.47	7.97	4.77
K_R (L g^{-1})	0.11					
n	0.26					
a_R (L $mmol^{-1}$)	6.13					
R^2	0.6546					
Sips		14.78	1.53	4.04	4.68	1.43
q_{max} (mmol g^{-1})	5.90					
q_{max} (mg g^{-1})	2,407					
K_s (L $mmol^{-1}$)	0.00					
n	1.13					
R^2	0.9617					

the Freundlich and the Temkin models can also be rejected. Of the two isotherm models left, even though the Sips model seemed to be not as closely fitted to the experiment data as the Langmuir model, as shown in Fig. 1, the Sips model has the highest R^2 value (>0.96) of all the six models used. In terms of overall errors, even though the Langmuir has the lower error values than the Sips, the difference in the error values between both models is not significant. Hence, based on highest R^2 and smallest error values, both the Sips and Langmuir models could be used to describe the adsorption of CV on CBGW, where the latter model corresponds to monolayer adsorption. The Sips model, on the other hand, is also known as the Langmuir–Freundlich isotherm model where it exhibits the characteristics of the Langmuir model at high adsorbate concentration and acts more to the Freundlich model at lower concentrations. The corresponding adsorption capacity (q_{max}) values of CBGW for CV determined from both models are 2,407 and 1,565 mg g^{-1}, respectively.

A large number of adsorbents have been reported in the literature for the removal of CV, and Table 4 lists some of these adsorbents (biosorbents and other adsorbents) together with their adsorption capacities. Although there has been a surge in the discovery of new adsorbents for the removal of pollutants, not all natural biosorbents are effective. Hence, alternatives have been searched upon in order to enhance adsorption capacity of adsorbents. One way is surface modification through chemical means, using various agents depending on the nature of the adsorbent and the adsorbate. For example, NaOH treated *A. camansi* peel has shown almost two-fold enhanced adsorption capacity toward CV. More sophisticated adsorbents such as nanocrystals and polymers, have also been attempted; however, their formations are usually complicated, and yet, the end products do not necessarily give good adsorption capacity, as reported in Table 4. As a natural adsorbent, untreated BGW has good q_{max} of 245 mg g^{-1} toward CV, which is better than some modified adsorbents. The cellulose derived BGW reported in this study greatly improves the adsorption capability of BGW, as observed by much higher q_{max} value of CBGW as an adsorbent, demonstrating its superiority when compared to many reported adsorbents.

Table 4
Adsorption capacity of selected adsorbents for the removal of CV reported in literature

Adsorbent	q_{max} (mg g^{-1})	Reference
Cellulose derived bitter gourd waste (Langmuir)	1,565	This study
(Sips)	2,407	This study
Bitter gourd waste	245	[14]
Cellulose oxidized from sugarcane bagasse	1,118	[29]
Carboxylate functionalized cellulose nanocrystals	244	[32]
Cellulose modified with maleic anhydride	34	[33]
Cellulose based adsorbent	219	[34]
Artocarpus odoratissimus skin – untreated	118	[23]
– NaOH treated	195	[23]
A. odoratissimus core	217	[35]
A. odoratissimus leaves	51	[36]
A. odoratissimus leaf-based cellulose	239	[37]
A. camansi (Breadnut) peel – untreated	275	[38]
– NaOH treated	479	[38]
Biopolymer-based magnetic beads	85	[39]
Montmorillonite – raw	370	[40]
– acid treated	400	[40]
Mango stone	353	[41]
Natural clay mineral	330	[42]
Artocarpus altilis skin	146	[43]
Alginate/acid activated bentonite beads	582	[44]
Peat	108	[45]

3.4. Adsorption kinetics

Investigation of kinetics of interaction of CV dye and CDBG can be performed using the Lagergren pseudo-first-order [46] and pseudo-second-order [47] models, whose linearized equations are shown below.

The linearized pseudo-first-order equation:

$$\log\left(q_e - q_t\right) = \log q_e - \frac{t}{2.303}k_1 \tag{2}$$

The linearized pseudo-second-order equation:

$$\frac{t}{q_t} = \frac{1}{q_e^2 k_2} + \frac{t}{q_e} \tag{3}$$

where q_t as well as q_e indicates the amount of CV adsorbed on CDBG at time t and at equilibrium, respectively, and k_1 and k_2 are the rate constants for the pseudo-first-order (min^{-1}) and the pseudo-second-order (g mg^{-1} min^{-1}), respectively.

Depending on the values of the R^2, errors, and the comparison between the experiment and calculated adsorption capacity (q_{exp} and q_{cal}, respectively), the relevant kinetics model can be ascertained. It is observed that kinetics is more in line with the pseudo-second-order based on the R^2 value being close to unity (Fig. 4). This is supported by the significantly lower error values for all five error types for the pseudo-second-order kinetics as shown in Table 5. Besides the R^2 and the error values, the q_{exp} and q_{cal} values for both CV concentrations are very close to each other in the pseudo-second-order kinetics model, as compared with the first-order where there is a huge difference. The validity of the pseudo-second-order kinetics can be further strengthened from the comparison of simulated non-linear kinetics plots for both the dye concentrations used in this study, as shown in Fig. 5. These plots show very clearly that unlike the pseudo-second-order kinetics, the pseudo-first-order is much deviated from the experiment data. This could be attributed to having two distinct adsorption sites on CDBG for CV molecules to be occupied differently.

3.5. Effect of ionic strength on adsorption of CV dye

Effect of the ionic strength of the medium on the extent of adsorption of CV by CBGW carried out using four different salts, namely KNO_3, KCl, $NaNO_3$, and NaCl, is shown in Fig. 6. It is clear from the Fig. 6 that adsorption of CV in the presence of NaCl remains quite high as much as 91% at 0.6 M ionic strength, in contrast to the untreated BGW whose adsorption has decreased as the concentration of NaCl increases [16]. For KCl, both BGW and CBGW show a similar trend in the adsorption of CV dye, but the extent of removal of CV by CBGW is higher than that of BGW, indicating that CBGW is more resilient to change in ionic strength. However, adsorption of CBGW decreases as the concentration of KNO_3 increases, especially at higher concentrations. Overall, it can be concluded that the change in the ionic strength of the medium up to 0.6 M does not have a significant impact on the extent of adsorption of CV.

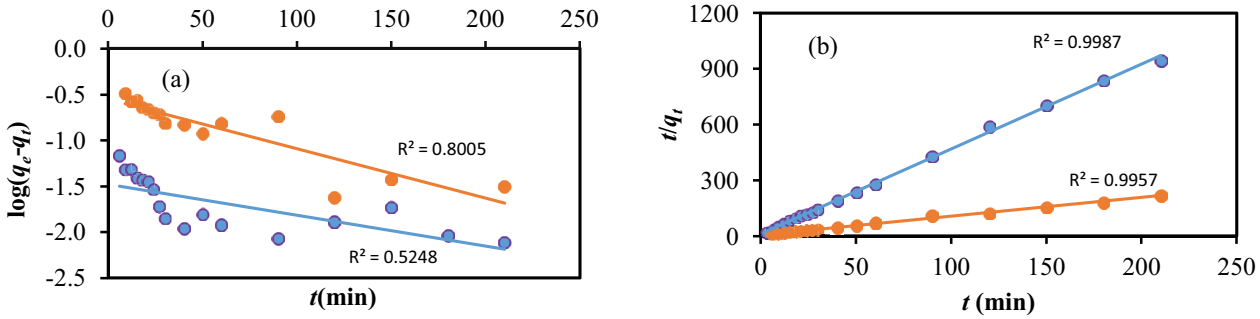

Fig. 4. Linear plots of (a) Lagergren pseudo-first and (b) pseudo-second-order kinetics for adsorption of CV on CDBG at different concentrations; 100 mg L^{-1} (●) and 500 mg L^{-1} (●).

Table 5
Comparison of parameters for pseudo-first and pseudo-second-order kinetics

Model	CV (mg L^{-1})	ARE	ERRSQ	HYBRID	EABS	χ^2	R^2	q_{cal} (mg g^{-1})	q_{exp} (mg g^{-1})
Pseudo-first-order	500	85.15	8.09	66.30	11.70	9.95	0.8045	0.30	1.21
	100	97.32	0.67	21.03	3.46	3.37	0.4605	0.03	0.19
Pseudo-second-order	500	12.98	0.29	2.37	1.77	0.35	0.9957	1.00	1.21
	100	7.24	0.01	0.20	0.25	0.03	0.9987	0.22	0.19

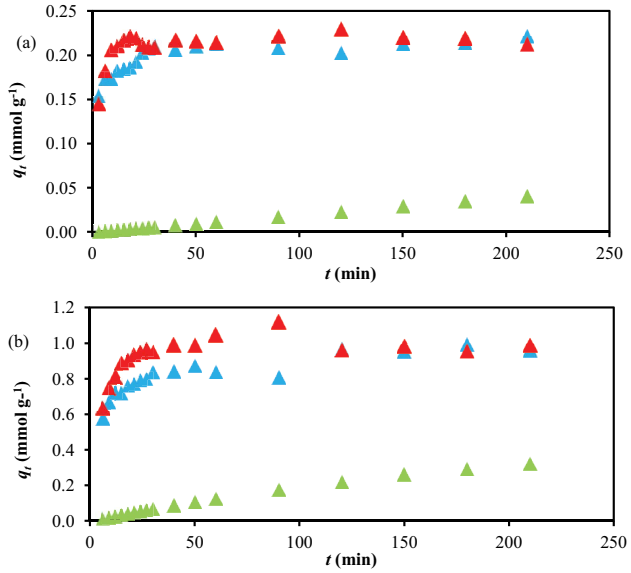

Fig. 5. Comparison of non-linear pseudo-first (▲) and pseudo-second-order (▲) kinetics with experiment data (▲) for different concentrations of CV adsorbed on CDBG (a) 100 mg L^{-1} CV and (b) 500 mg L^{-1} CV.

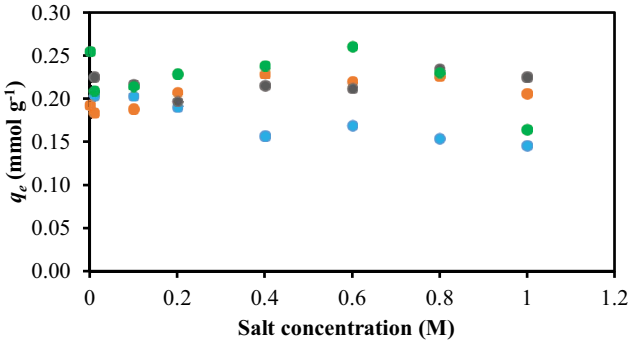

Fig. 6. Extent of removal of CV dye from 100 mg L^{-1} solutions by CBGW at different strengths of KNO_3 (●), KCl (●), $NaNO_3$ (●), and NaCl (●) (10.0 mL dye solution; 20 mg CBGW; 210 min shaking time; 250 rpm shaking speed).

It is reported that NaCl significantly enhances the dissolution and depolymerization of cellulose [48]. The presence of NaCl thus shows two opposing effects; dissolution will make the adsorbent unstable thus lowering the adsorption behavior. On the other hand, depolymerization would promote adsorption as polymeric chains are opened up. Further, Cl^- could interact strongly with the end $^-$OH groups of glucose, resulting in enhanced breaking of both inter- and intra-molecular hydrogen bonds. This would also promote adsorption due to opening of long chains in the cellulose molecule. Increase in the extent or removal of CV in the presence of KCl, $NaNO_3$, and NaCl up to the ionic strength of 0.6 M can thus be attributed to depolymerization and breaking of hydrogen bonds. Decrease in the extent of adsorption in NaCl solutions beyond 0.6 M ionic strength could be due to dissolution effect. Lower extents of removal in KNO_3 solutions would probably be due to competition of K^+ and positively charged CV dye molecules for the same adsorption sites.

3.6. Regeneration of CBGW

Fig. 7 illustrates that the percentage of the CV dye removed from the spent CBGW drastically reduced with

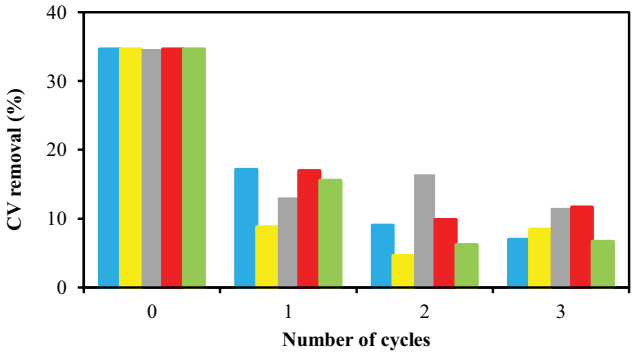

Fig. 7. Adsorption of CV with successive cycles of regeneration with different media [washed with distilled water (■), quick rinse with distilled water (■), 0.1 M NaOH (■), 0.1 M HCl (■), and control (■)].

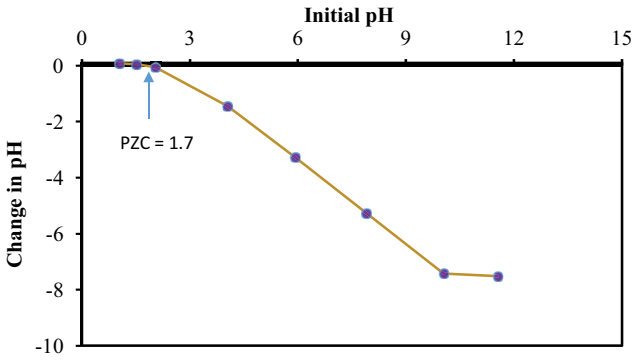

Fig. 8. Variation of change in pH of the aqueous KNO_3 suspensions of CBGW with initial pH.

increasing number of cycles. Among many reagents used, acid or base treatment of the spent CBGW appears to be the best, as compared to washing or rinsing with water and the control experiment. Regeneration was not attempted beyond the third consecutive cycle since the release of CV dye dropped to <12%. However, it must be highlighted that unlike for other literature reports where low dye concentrations were used, in this study a very high concentration of 2,000 mg L^{-1} was used. Hence, the ability of spent CBGW to sustain three consecutive cycles to great extent once again demonstrates the superiority of CBGW as an adsorbent for CV dye.

3.7. Characterization CBGW

Change in pH vs. initial pH curve crosses the axis at pH = 1.66 at which the surface of the adsorbent is neutral, which is the point of zero charge of CBGW (Fig. 8). At pH > 1.66, deprotonation causes the surface to be more negatively charged. This in turn will lead to greater electrostatic attraction between the negatively charged surface and the cationic CV dye molecules. This prediction is in fact in line with what was observed in this study. In comparison for the removal of dye at lower pH, a slight decrease in % removal was observed due to the surface of the adsorbent gaining moving toward neutrality, resulting in decreased electrostatic attraction towards CV.

The change in surface morphology, before and after chemical treatment of BGW to obtain CBGW, can be clearly observed from the SEM images as shown in Fig. 9. Prior to treatment, the surface of BGW appears more densely packed whereas CBGW seemed to have larger and more prominent cavities and pores, when observed under the same magnification. This probably explains the effect of increased surface area on enhanced adsorption ability in addition to other chemical changes promoting attraction of CV dye molecules, as shown by its high q_{max} value. It is also interesting to note that when CBGW was treated with CV dye, its surface becomes completely changed, filling with spikes of crystals, as shown in Fig. 9c.

Vibrational bands observed from the IR spectrum of the extracted cellulose includes C–O stretching (1,057 cm^{-1}), C–O–C stretching of the β-(1,4)-glycosidic linkages (1,152 cm^{-1}), C–O–H in-plane bending (1,209 cm^{-1}), C–C stretching (1,418 cm^{-1}), C–O stretching (1,614 cm^{-1}), C–H asymmetric stretching (2,852 cm^{-1}), C–H symmetric stretching (2,913 cm^{-1}), and O–H stretching (3,344 cm^{-1}). As seen from Fig. 10, generally the peak intensities for the CBGW are lowered when CV is adsorbed on its surface. The most prominent difference is the value in between 3,300 and 3,500 cm^{-1} which indicates that the N–H group present in the CBGW is involved in adsorption, and hence decrease in the intensity is observed in response with the CV dye. The C=O bond is also contributed to the adsorption process as seen by the loss of intensity of the peak at around 1,750 cm^{-1}.

4. Conclusion

CBGW obtained using a simple method of refluxing BGW with a mixture of acetic acid and nitric acid, can be successfully utilized as a new adsorbent for the removal of Crystal violet dye (CV) from simulated wastewater. Its superior adsorption capacity toward Crystal violet dye, as much as 1,565 mg g^{-1} (Langmuir adsorption isotherm) and 2,407 mg g^{-1} (Sips adsorption isotherm), determined in adsorption systems in batch mode under optimized laboratory conditions, to most reported adsorbents indicates its potential application in real-life wastewater treatment after further optimization and adjustments for dynamic conditions. Adsorption of CV dye on CBGW follows pseudo-second-order kinetics indicating that there are two distinct adsorption sites available on the adsorbent surface, and further salts present in the adsorbate medium would lead to depolymerization, breaking up of hydrogen bonding, and solubilization of cellulose with different extents depending on the specific types of ions present. The spent CBGW is able to release very high dye concentration for a few cycles, indicating its ability to be regenerated and reused. Generally, CBGW was resilient to ionic strength up to 0.20 M and medium pH, further adding to its attractiveness as a low-cost adsorbent.

Acknowledgments

We the authors hereby would like to thank the Government of Brunei Darussalam and the Universiti Brunei Darussalam for their continual support.

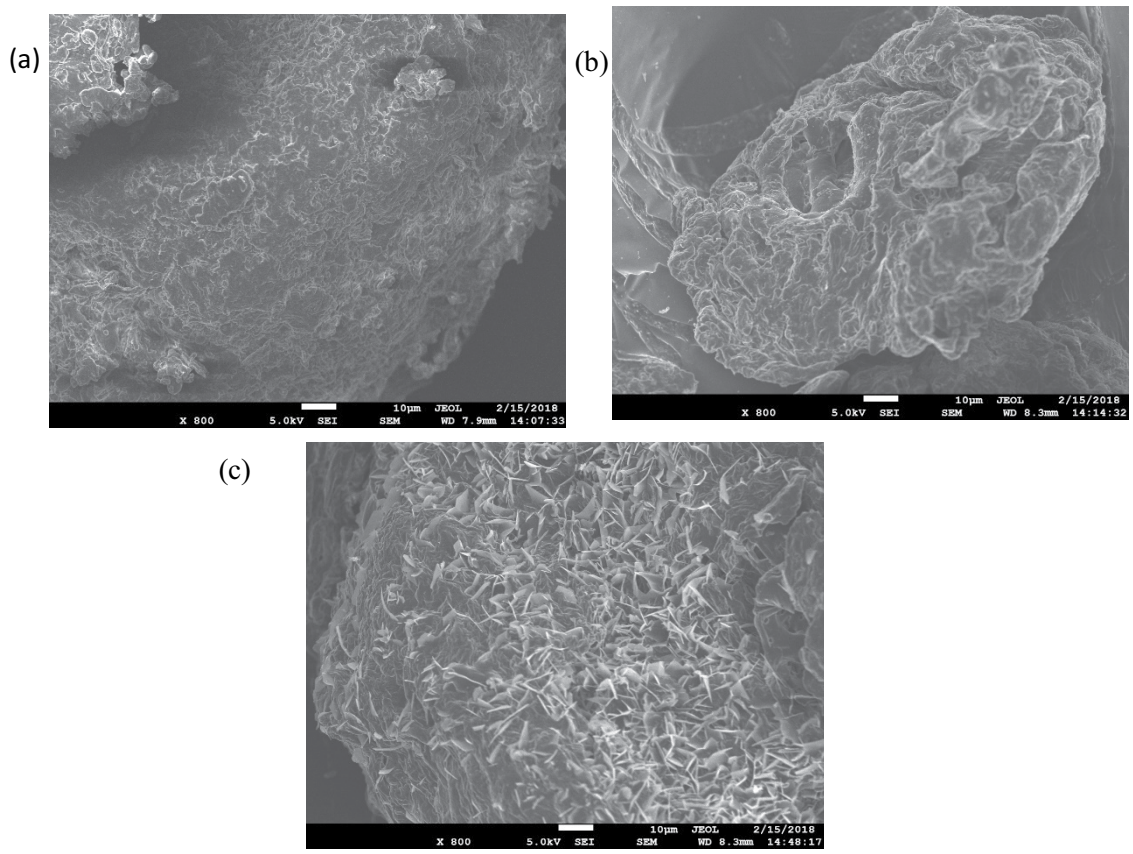

Fig. 9. SEM images of (a) BGW, (b) CBGW, and (c) CBGW loaded with CV dye, at 800× magnification with scale bar representing 10 μm.

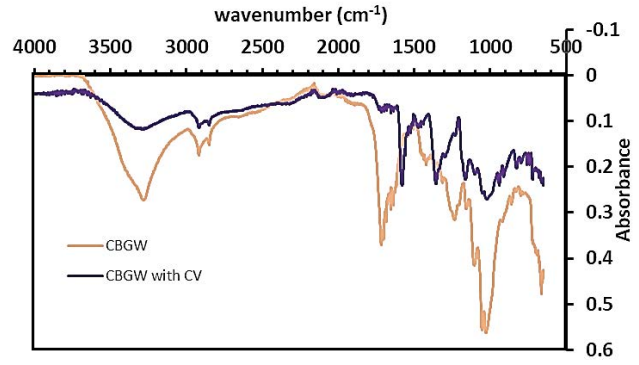

Fig. 10. FTIR spectra of CBGW and CBGW with CV.

References

[1] D. Hoornweg, P. Bhada-Tata, C. Kennedy, Environment: waste production must peak this century, Nat. News, 502 (2013) 615–617.
[2] S. Shams, R.H.M. Juani, Z. Guo, Integrated and Sustainable Solid Waste Management for Brunei Darussalam, 5th Brunei International Conference on Engineering and Technology (BICET 2014), Bandar Seri Begawan, Brunei, 2014.
[3] C. Cooksey, Hematoxylin and related compounds–an annotated bibliography concerning their origin, properties, chemistry, and certain applications, Biotech. Histochem., 85 (2010) 65–82.
[4] F.M.D. Chequer, G.A.R.D. Oliveira, E.R.A. Ferraz, J.C. Cardoso, M.V.B. Zanoni, D.P.D. Oliveira, Textile Dyes: Dyeing Process and Environmental Impact, Melih Günay, Ed., Eco-Friendly Textile Dyeing and Finishing, InTech Publishers, 2013, pp. 151–169. Available at: https://www.intechopen.com/books/eco-friendly-textile-dyeing-and-finishing/textile-dyes-dyeing-process-and-environmental-impact
[5] B. de Campos Ventura-Camargo, B. Marin-Morales, M. Aparecida, Azo dyes: characterization and toxicity – a review, Text. Light Ind. Sci. Technol., 2 (2013) 85–103.
[6] H.B. Mansour, I. Houas, F. Montassar, K. Ghedira, D. Barillier, R. Mosrati, L. Chekir-Ghedira, Alteration of *in vitro* and acute *in vivo* toxicity of textile dyeing wastewater after chemical and biological remediation, Environ. Sci. Pollut. Res., 19 (2012) 2634–2643.
[7] J. Wang, Y. Shih, P.Y. Wang, Y.H. Yu, J.F. Su, C. Huang, Hazardous waste treatment technologies, Water Environ. Res., 91 (2019) 1177–1198.
[8] C.R. Holkar, A.J. Jadhav, D.V. Pinjari, N.M. Mahamuni, A.B. Pandit, A critical review on textile wastewater treatments: possible approaches, J. Environ. Manage., 182 (2016) 351–366.
[9] Y. Safa, H.N. Bhatti, Adsorptive removal of direct textile dyes by low cost agricultural waste: application of factorial design analysis, Chem. Eng. J., 167 (2011) 35–41.
[10] D. Bulgariu, L. Bulgariu, Equilibrium and kinetics studies of heavy metal ions biosorption on green algae waste biomass, Bioresour. Technol., 103 (2012) 489–493.
[11] L.B.L. Lim, N. Priyantha, N.A.H.M. Zaidi, U.A.N. Jamil, H.I. Chieng, T. Zehra, A. Liyandeniya, Chemical modification of *Artocarpus odoratissimus* skin for enhancement of their adsorption capacities toward toxic malachite green dye, J. Mater. Environ. Sci., 7 (2016) 3211–3224.
[12] L. Bulgariu, L.B. Escudero, O.S. Bello, M. Iqbal, J. Nisar, K.A. Adegoke, F. Alakhras, M. Kornaros, I. Anastopoulos,

The utilization of leaf-based adsorbents for dyes removal: a review, J. Mol. Liq., 276 (2019) 728–747.
[13] G. Selvakumar, G. Shathirapathiy, R. Jainraj, P.Y. Paul, Immediate effect of bitter gourd, ash gourd, Knol-khol juices on blood sugar levels of patients with type 2 diabetes mellitus: a pilot study, J. Traditonal Complementary Med., 7 (2017) 526–531.
[14] L.B.L. Lim, N. Priyantha, K.J. Mek, N.A.H.M. Zaidi, Potential use of *Momordica charantia* (bitter gourd) waste as a low-cost adsorbent to remove toxic Crystal violet dye, Desal. Water Treat., 82 (2017) 121–130.
[15] S. Akhtar, Q. Husain, Potential applications of immobilized bitter gourd (*Momordica charantia*) peroxidase in the removal of phenols from polluted water, Chemosphere, 65 (2006) 1228–1235.
[16] R. Docampo, S.N.J. Moreno, The metabolism and mode of action of gentian violet, Drug Metab. Rev., 22 (1990) 161–178.
[17] T. Hashimoto, M. Ohori, T. Kashima, H. Yamamoto, M. Tachibana, Chemical cystitis due to Crystal violet dye: a case report, J. Med. Case Rep., 7 (2013) 145, doi: 10.1186/1752-1947-7-145.
[18] S. Hokkanen, A. Bhatnagar, M. Sillanpaa, A review on modification methods to cellulose-based adsorbents to improve adsorption capacity, Water Res., 91 (2016) 156–173.
[19] X. Zheng, X. Li, J. Li, L. Wang, W. Jin, Y. Pei, K. Tang, Efficient removal of anionic dye (Congo red) by dialdehyde microfibrillated cellulose/chitosan composite film with significantly improved stability in dye solution, Int. J. Biol. Macromol., 107 (2018) 283–289.
[20] F. Jiang, D.M. Dinh, Y.-L. Hsieh, Adsorption and desorption of cationic malachite green dye on cellulose nanofibril aerogels, Carbohydr. Polym., 173 (2017) 286–294.
[21] L.R. Martins, J.A.V. Rodrigues, O.F.H. Adarme, T.M.S. Melo, L.V.A. Gurgel, L.F. Gil, Optimization of cellulose and sugarcane bagasse oxidation: Application for adsorptive removal of Crystal violet and auramine-O from aqueous solution. J. Colloid Interface Sci., 494 (2017) 223–241.
[22] G.J. Kulić, V.B. Radojičić, Analysis of cellulose content in stalks and leaves of large leaf tobacco, J. Agric. Sci. Belgrade, 56 (2011) 207–215.
[23] L.B.L. Lim, N. Priyantha, T. Zehra, C.W. Then, C.M. Chan, Adsorption of Crystal violet dye from aqueous solution onto chemically treated *Artocarpus odoratissimus* skin: equilibrium, thermodynamics, and kinetics studies, Desal. Water Treat., 57 (2016) 10246–10260.
[24] K.Z. Elwakeel, A.M. Elgarahy, G.A. Elshoubaky, S.H. Mohammad, Microwave assist sorption of Crystal violet and Congo red dyes onto amphoteric sorbent based on upcycled Sepia shells, J. Environ. Health Sci. Eng., 18 (2020) 35–50.
[25] A.H. Abd El-Salam, H.A. Ewais, A.S. Basaleh, Silver nanoparticles immobilised on the activated carbon as efficient adsorbent for removal of Crystal violet dye from aqueous solutions. A kinetic study, J. Mol. Liq., 248 (2017) 833–841.
[26] I. Langmuir, The adsorption of gases on plane surfaces of glass, mica and platinum, J. Am. Chem. Soc., 40 (1918) 1361–1403.
[27] H. Freundlich, Over the adsorption in the solution, J. Phys. Chem., 57 (1906) 385–470.
[28] M. Temkin, V. Pyzhev, Kinetics of ammonia synthesis on promoted iron catalyst, Acta Physicochim. U.R.S.S., 12 (1940) 327–356.
[29] M.M. Dubinin, L.V. Radushkevich, The equation of the characteristic curve of the activated charcoal, Proc. Acad. Sci. Phys. Chem. Sect., 55 (1947) 331–337.
[30] R. Sips, On the structure of a catalyst surface, J. Chem. Phys., 16 (1948) 490–495.
[31] O. Redlich, D.L. Peterson, A useful adsorption isotherm, J. Phys. Chem., 63 (1959) 1024–1024.
[32] H. Qiao, Y. Zhou, F. Yu, E. Wang, Y. Min, Q. Huang, L. Pang, T. Ma, Effective removal of cationic dyes using carboxylate-functionalized cellulose nanocrystals, Chemosphere, 141 (2015) 297–303.
[33] Y. Zhou, Q. Jin, X. Hu, Q. Zhang, T. Ma, Heavy metal ions and organic dyes removal from water by cellulose modified with maleic anhydride, J. Mater. Sci., 47 (2012) 5019–5029.
[34] Y. Zhou, M. Zhang, X. Wang, Q. Huang, Y. Min, T. Ma, J. Niu, Removal of Crystal violet by a novel cellulose-based adsorbent: comparison with native cellulose, Ind. Eng. Chem. Res., 53 (2014) 5498–5506.
[35] M.K. Dahri, M.R.R. Kooh, L.B.L. Lim, *Artocarpus odoratissimus* (Tarap) core as an adsorbent for the removal of Crystal violet dye from aqueous solution, J. Mater. Environ. Sci., 8 (2017) 3706–3717.
[36] L.B.L. Lim, N. Priyantha, H.H. Cheng, N.A.H.M. Zaidi, Adsorption characteristics of *Artocarpus odoratissimus* leaf toward removal of toxic Crystal violet dye: isotherm, thermodynamics and regeneration studies, J. Environ. Biotechnol. Res., 4 (2016) 32–40.
[37] N.A.H.M. Zaidi, L.B.L. Lim, A. Usman, *Artocarpus odoratissimus* leaf-based cellulose as adsorbent for removal of Methyl violet and Crystal violet dyes from aqueous solution, Cellulose, 25 (2018) 3037–3049.
[38] H.I. Chieng, L.B.L. Lim, N. Priyantha, Enhancement of Crystal violet dye adsorption on *Artocarpus camansi* peel through sodium hydroxide treatment, Desal. Water Treat., 58 (2017) 320–331.
[39] G.R. Mahdavinia, S. Iravani, S. Zoroufi, H. Hosseinzadeh, Magnetic and K^+-cross-linked kappa-carrageenan nanocomposite beads and adsorption of Crystal violet, Iran. Polym. J., 23 (2014) 335–344.
[40] G.K. Sarma, S.S. Gupta, K.G. Bhattacharyya, Adsorption of Crystal violet on raw and acid-treated montmorillonite, K_{10}, in aqueous suspension, J. Environ. Manage., 171 (2016) 1–10.
[41] S. Shoukat, H.N. Bhatti, M. Iqbal, S. Noreen, Mango stone biocomposite preparation and application for Crystal violet adsorption: a mechanistic study, Microporous Mesoporous Mater., 239 (2017) 180–189.
[42] O.S. Omer, M.A. Hussein, B.H. Hussein, A. Mgaidi, Adsorption thermodynamics of cationic dyes (methylene blue and Crystal violet) to a natural clay mineral from aqueous solution between 293.15 and 323.15 K, Arabian J. Chem., 11 (2018) 615–623.
[43] L.B.L. Lim, N. Priyantha, N.H.M. Mansor, *Artocarpus altilis* (breadfruit) skin as a potential low-cost biosorbent for the removal of Crystal violet dye: equilibrium, thermodynamics and kinetics studies, Environ. Earth Sci., 73 (2015) 3239–3247.
[44] A.A. Oladipo, M. Gazi, Enhanced removal of Crystal violet by low cost alginate/acid activated bentonite composite beads: optimization and modelling using non-linear regression technique, J. Water Process Eng., 2 (2014) 43–52.
[45] H.I. Chieng, L.B.L. Lim, N. Priyantha, D.T.B. Tennakoon, Sorption characteristics of peat of Brunei Darussalam III: equilibrium and kinetics studies on adsorption of Crystal violet (CV), Int. J. Earth Sci. Eng., 6 (2013) 791–801.
[46] S. Lagergren, About the theory of so-called adsorption of soluble substances, Kungl. Svens. Vetenskapsakad. Handl., 24 (1898) 1–39.
[47] Y.S. Ho, G. McKay, Sorption of dye from aqueous solution by peat, Chem. Eng. J., 70 (1998) 115–124.
[48] Z. Jiang, J. Yi, J. Li, T. He, C. Hu, Promoting effect of sodium chloride on the solubilization and depolymerization of cellulose from raw biomass materials in water, ChemSusChem, 8 (2015) 1901–1907.